ARCHIVES OF THE TURKISH SOCIETY OF CARDIOLOGY

TURKISH SOCIETY OF CARDIOLOGY

Differences in fractional flow reserve derived from coronary computed tomography angiography according to coronary artery bifurcation angle

Bilgisayarlı tomografik anjiyografi ile elde edilen orantısal akım yedeğinin koroner arter bifürkasyon açısına göre farklılıkları

CASE IMAGE
OLGU GÖRÜNTÜSÜ

Computed tomography (CT) derived fractional flow reserve (FFR_{CT}) decreases from proximal to distal part of the left coronary artery under the influence of various factors. The energy loss owing to the bifurcation angle may contribute to progressive FFR_{CT} decline. However, the effect of bifurcation angle on FFR_{CT} is unclear.

CASE REPORT

Case 1

This was a 60-year-old man whose CT angiography (CTA) revealed no significant coronary artery stenosis in the left-main-coronary trunk (LMT), left-anterior-descending (LAD), and left-circumflex (LCX). Vessel length was 111.2 mm for LAD and 62.5 mm for LCX (Figure 1A). Three-dimensional volume-rendered image of the coronary tree showed that the LMT-LAD-LCX bifurcation angle was 123.1° (Figure 2A). FFR_{CT} at LCX just after the LMT-LAD-LCX bifurcation was 0.95 and gradually decreased to 0.90 at its distal portion, whereas at LAD just after the LMT-LAD-LCX bifurcation was 0.96 and dropped to 0.75 at its distal portion. (Fig. 3A). Invasive coronary angiography showed no significant coronary artery stenosis in the LMT, LAD, and LCX as well as in CTA (Figure 4A and Video 1*, 2*). However, invasive FFR value of 0.88 at the distal LAD was inconsistent with FFR_{CT} of 0.75.

Case 2

This was a 59-year-old man with CTA revealing no significant coronary artery stenosis in the LMT, LAD, and LCX. Vessel length was 110.6 mm for LAD and 62.5 mm for LCX (Figure 1B). Three-dimensional volume rendered image of the coronary tree showed that the LMT-LAD-LCX bifurcation angle was 54.3° (Figure 2B). FFR_{CT} at LAD and LCX just after the

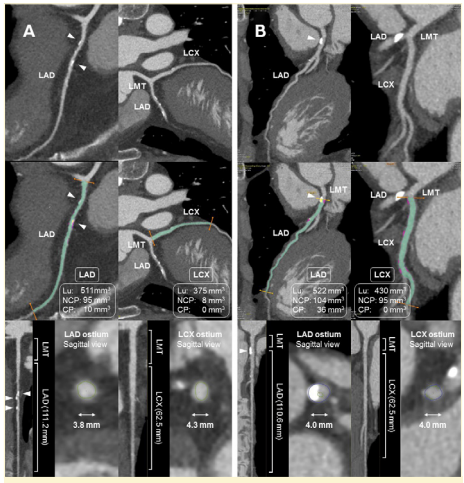

Figure 1. Computed tomography angiography (CTA): (A) Case 1; CTA showing no significant coronary artery stenosis in the left main trunk (LMT), left anterior descending (LAD), and left circumflex (LCX) (upper panel). Vessel components are indicated as following colors: green is lumen volume (Lu), red is non-calcified plaque volume (NCP), and yellow is calcified plaque volume (CP). The volume of Lu, NCP, and CP are 511 mm^3, 95 mm^3, and 10 mm^3 for LAD and 375 mm^3, 8 mm^3, and 0 mm^3 for LCX, respectively (middle panel). The vessel length coinciding with FFR_{CT} region of interest and ostium lumen diameter are 111.2 mm and 3.8 mm for LAD and 62.5 mm and 4.3 mm, respectively (lower panel). (B) Case 2; CTA showing no significant coronary artery stenosis in the LMT, LAD, and LCX (upper panel). The volume of Lu, NCP, and CP are 522 mm^3, 104 mm^3, and 36 mm^3 for LAD and 430 mm^3, 95 mm^3, and 0 mm^3 for LCX, respectively (middle panel). The vessel length coinciding with FFR_{CT} region of interest and ostium lumen diameter are 110.6 mm and 4.0 mm for LAD and 62.5 mm and 4.0 mm, respectively (lower panel). Arrowhead indicates CP.

Toshimitsu Tsugu, M.D.
Kaoru Tanaka, M.D.

Department of Radiology, Universitair Ziekenhuis Brussel, Brussels, Belgium

Corresponding Author:
Toshimitsu Tsugu
✉ tsugu917@gmail.com

Received: May 3, 2021
Accepted: August 9, 2021

Cite this article as: Tsugu T, Tanaka K. Differences in fractional flow reserve derived from coronary computed tomography angiography according to coronary artery bifurcation angle. Turk Kardiyol Dern Ars 2022;50:83-4.

DOI: 10.5543/tkda.2022.21104

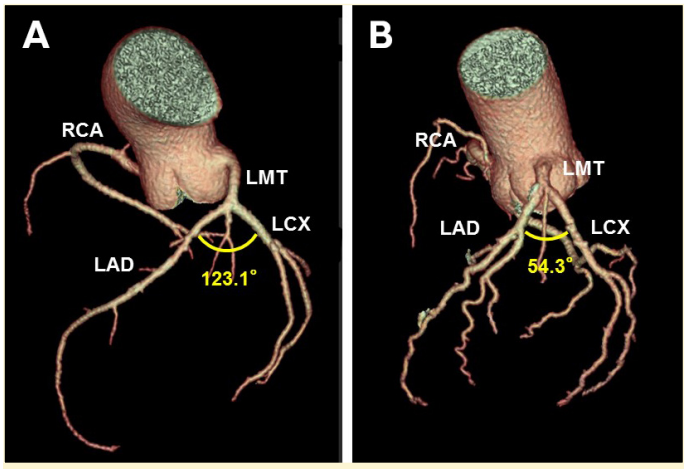

Figure 2. Three dimensional volume rendered image of the coronary tree. (A) Case 1: The LMT-LAD-LCX bifurcation angle is 123.1°. (B) Case 2: The LMT-LAD-LCX bifurcation angle is 54.3°.
LAD: left anterior descending; LCX: left circumflex; LMT: left main trunk; RCA: right coronary artery.

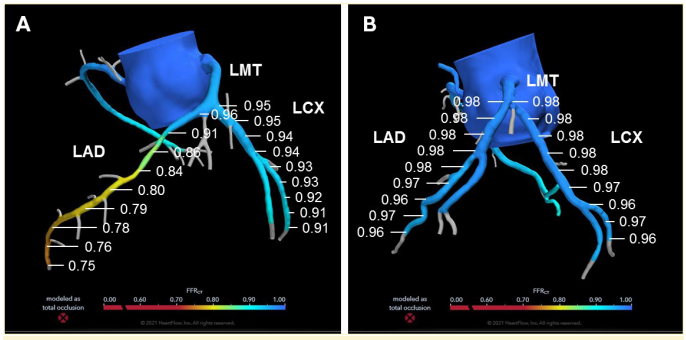

Figure 3. Computed tomography angiography derived fractional flow reserve (FFR_{CT}). (A) Case 1: FFR_{CT} is 0.96 at LAD just after the LMT-LAD-LCX bifurcation and decreases to 0.75 at its distal portion. FFR_{CT} is 0.95 at the LCX just after the LMT-LAD-LCX bifurcation and decreases to 0.91 at its distal portion. (B) Case 2: FFR_{CT} is 0.98 at LAD just after the LMT-LAD-LCX bifurcation and decreases to 0.96 at its distal portion. FFR_{CT} is 0.98 at LAD just after the LMT-LAD-LCX bifurcation and gradually decreases to 0.96 at its distal portion.
LAD: left anterior descending; LCX: left circumflex; LMT: left main trunk.

LMT-LAD-LCX bifurcation was 0.98 with a slight decrease to 0.96 for both vessels at its distal portion (Figure 3B). Invasive coronary angiography showed no significant coronary artery stenosis in LMT, LAD, and LCX, same as CTA (Figure 4B and Videos 3*, 4*).

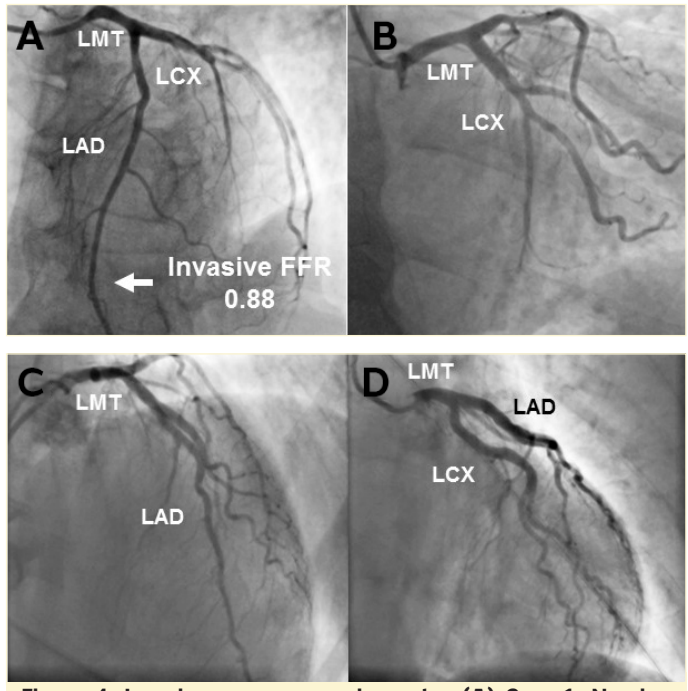

Figure 4. Invasive coronary angiography. (A) Case 1: No significant coronary artery stenosis in the LMT, LAD, and LCX. (B) Case 2: No significant coronary artery stenosis in the LMT, LAD, and LCX.
LAD: left anterior descending; LCX: left circumflex; LMT: left main trunk.

Left coronary artery bifurcation angle is known to affect the wall shear stress and cause disturbances of the bloodstream. Significant disturbance of laminar flow can contribute to FFR decline beyond established factors such as lumen narrowing or lesion length. The patients we have presented here confirmed that there was no significant coronary artery stenosis in both LAD and LCX by CTA and ICA. Moreover, vessel length and lumen volume were almost similar in LAD and LCX. These findings suggest that left coronary artery bifurcation angle influences the hemodynamic changes to the left coronary arteries and may have a potential to affect the FFR_{CT}. To the best of our knowledge, this is the first report of the effects of bifurcation angle on FFR_{CT}. The cases highlighted here suggest that the wide bifurcation angle could influence FFR_{CT} decline owing to the shear stress resulting in energy loss.

Written informed consent was obtained from the patients for the publication of the case image and the accompanying images.

*Supplementary video files associated with this article can be found in the online version of the journal.